

05:09:12

## Увеличение чувствительности спектрометра электронного парамагнитного резонанса с помощью сегнетоэлектрического резонатора

© И.Н. Гейфман,<sup>1</sup> И.С. Головина,<sup>1</sup> Е.Р. Зусманов,<sup>1</sup> В.И. Кофман<sup>2</sup>

<sup>1</sup> Институт физики полупроводников АН Украины,  
252650 Киев, Украина

<sup>2</sup> Североизападный университет, Эванстон, США

(Поступило в Редакцию 26 августа 1998 г. В окончательно редакции 8 февраля 1999 г.)

Для увеличения чувствительности радиоспектрометров ЭПР предложено использовать сегнетоэлектрический материал в качестве дополнительного резонатора. Метод опробован на радиоспектрометре ЭПР РЭ-1307 и на импульсном радиоспектрометре. Рассмотрены возможности увеличения соотношения сигнал/шум для сегнетоэлектрического резонатора прямоугольной и сферической форм. При использовании прямоугольного сегнетоэлектрического резонатора из tantalата калия достигнуто увеличение соотношения сигнал/шум в 16 раз при 331 К и в 10 раз при 292 К. В импульсном эксперименте присутствие сегнетоэлектрического резонатора позволило уменьшить СВЧ мощность, необходимую для насыщения образца, в 50 раз при 50 К.

Метод электронного парамагнитного резонанса (ЭПР) широко используется в физике, химии, медицине, биологии и в других областях знаний. На начальном этапе развития этого метода исследования проводились главным образом на специально приготовленных образцах, в которые в качестве парамагнитного зонда вводилась примесь. В настоящее время методом ЭПР исследуются естественные (иследованные) объекты, в которых концентрация парамагнитных центров часто оказывается недостаточной для наблюдения сигнала ЭПР. Поэтому исследователями предпринимаются попытки увеличить чувствительность радиоспектрометра. Одним из простейших способов увеличения соотношения сигнал/шум является введение в резонатор диэлектрического материала. Так, в [1] использовалась кварцевая пластина. Размещение образца вблизи пластины приводило к увеличению соотношения сигнал/шум в 4.5 раза. Также были использованы сегнетоэлектрические резонаторы из  $TiO_2$  [2,3] и  $SrTiO_3$  [4], однако их форма не позволяла исследовать ЭПР других материалов.

Детальное исследование влияния диэлектрической жидкости на ЭПР, как непрерывный (CW), так и импульсный, проведено в [5]. Установлено, что сигнал пропорционален квадрату напряженности СВЧ поля на образце, если изменение СВЧ поля связано с положением образца в резонаторе.

При регистрации сигналов спинового эха необходимо применение усилителей СВЧ мощности. Это связано с тем, что производство падающей мощности СВЧ на длину импульса в спиновом эхе определяет поворот намагниченности ( $\pi/2$  или  $\pi$ ). Используемые импульсы являются избирательными, если их длительность превышает 7–10 нс. Для избирательных  $\pi$ -импульсов, применяемых, например, в двумерном HYSCORE (Hyperfine Sublevel Correlation Experiment), требуется большая мощность, так что предлагаемый в настоящей работе сег-

нетоэлектрический материал может заменить усилитель СВЧ мощности (либо позволить использовать усилитель СВЧ меньшей мощности).

В настоящей работе изучено влияние наличия в объемном цилиндрическом резонаторе сегнетоэлектрического резонатора на интенсивность сигнала обычного (CW) ЭПР и на сигнал спинового эха (ESEEM).

### 1. Влияние сегнетоэлектрического резонатора на сигнал CW ЭПР

Измерения проводились на радиоспектрометре ЭПР РЭ-1307 с высокочастотной модуляцией магнитного поля в трехсантиметровом (X band) диапазоне длии волн в температурном интервале 220–370 К. Сегнетоэлектрический резонатор размещался в центре объемного цилиндрического резонатора с типом волны  $TE_{011}$ . Изготовлены два сегнетоэлектрических резонатора из монокри-

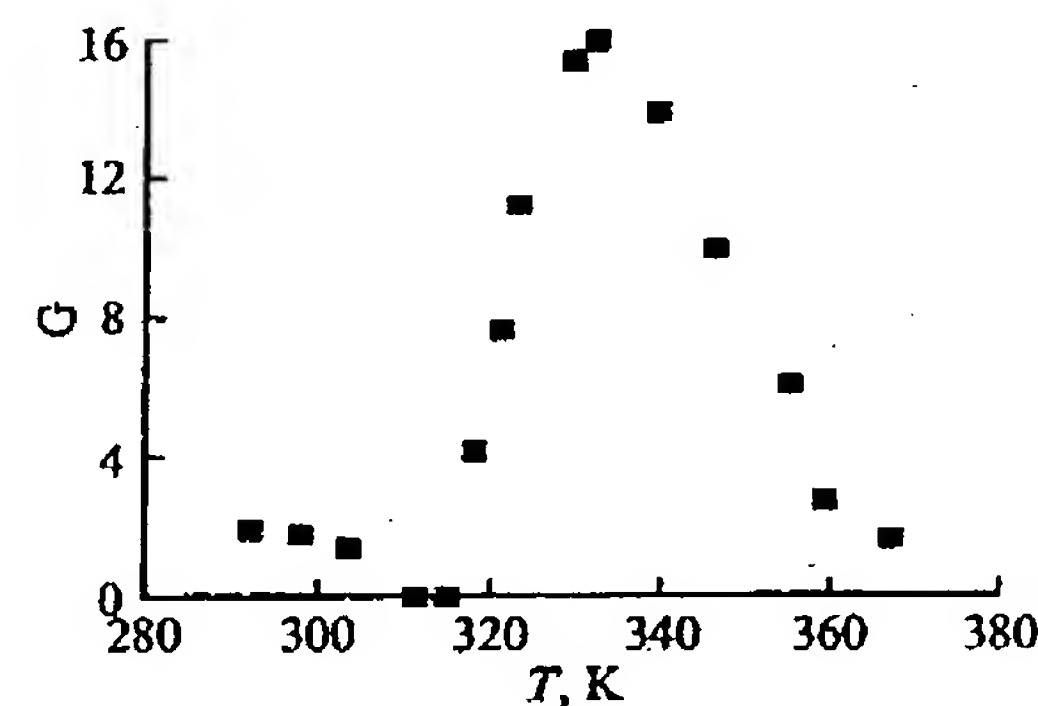
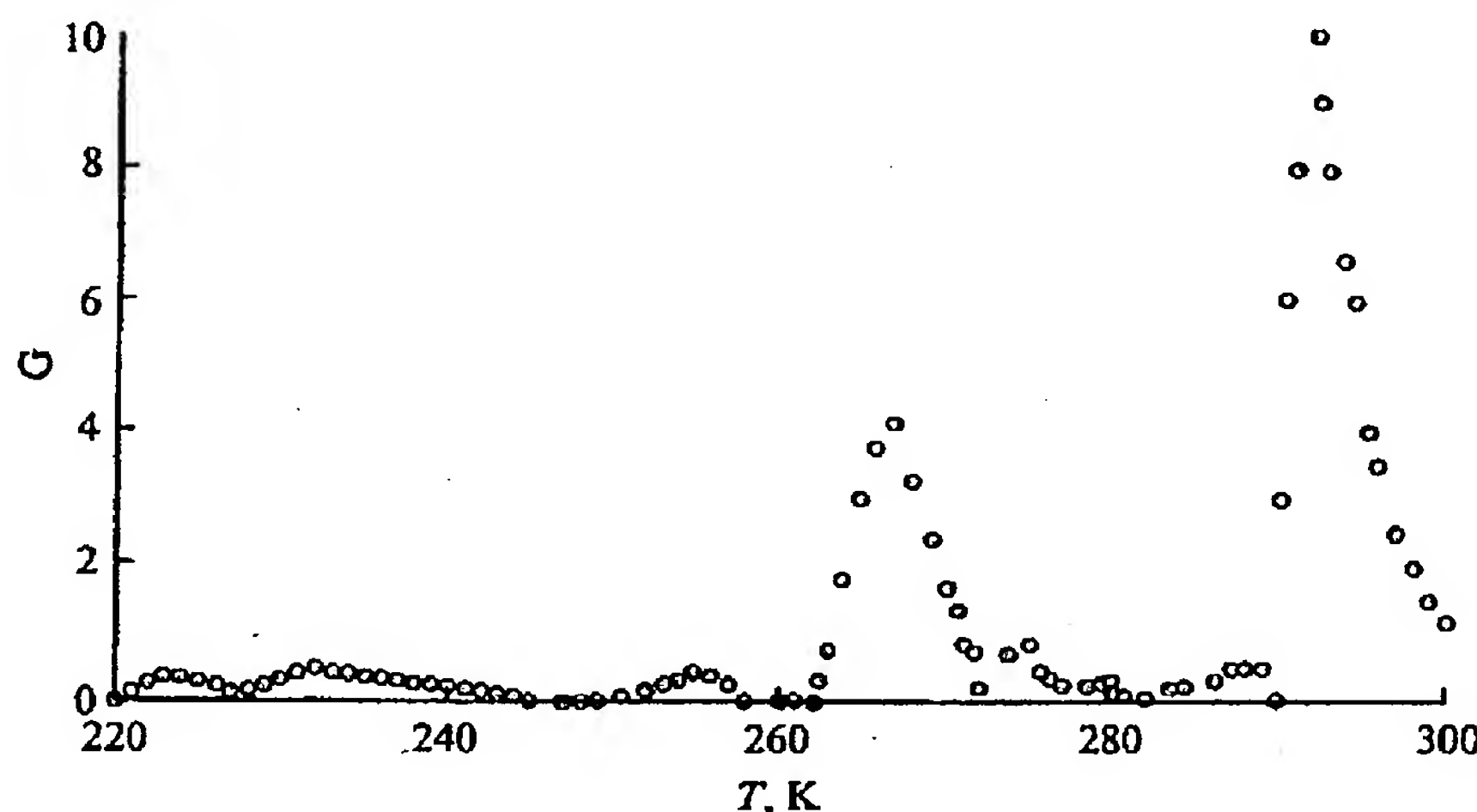


Рис. 1. Температурная зависимость увеличения соотношения сигнал/шум  $G$  при размещении образца в сегнетоэлектрическом резонаторе I.

122

*И.Н. Гейфман, И.С. Головина, Е.Р. Зусманов, В.И. Кофман*



**Рис. 2.** Температурная зависимость увеличения соотношения сигнал/шум  $S$  при размещении образца в сегнетоэлектрическом резонаторе II.

сталического танталата калия ( $\text{KTaO}_3$ ), каждый из них представлял собой четырехгранную призму размсром  $2.85 \times 2.6 \times 3.4 \text{ mm}$  (I) и  $2.75 \times 3.5 \times 4.6 \text{ mm}$  (II). В качестве материала для сегнетоэлектрического резонатора выбран танталат калия благодаря его уникальным свойствам; в частности, это единственный материал, у которого с ростом диэлектрической проницаемости уменьшаются диэлектрические потери [6]. По центру призмы высверлено отверстие радиусом  $R = 0.9 \text{ mm}$  и глубиной  $h = 2$  и  $4 \text{ mm}$  для резонаторов I и II соответственно. В это отверстие помещался образец — дифенил пикрил гидразил (ДФПГ), находящийся в кварцевой ампуле диаметром 1 mm. Сегнетоэлектрический резонатор размещался в объемном резонаторе таким образом, что ось высверленного отверстия совпадала с силовыми линиями магнитной компоненты СВЧ поля.

Наличие сегнетоэлектрического резонатора в объемном резонаторе увеличивает соотношение сигнал/шум. Так, размещение образца в резонаторе I приводит к увеличению соотношения сигнал/шум в 16 раз при температуре 331 К (рис. 1) и в 10 раз при 292 К при размещении образца в резонаторе II (рис. 2). Как видно из рис. 1 и 2, изменение соотношения сигнал/шум в присутствии сегнетоэлектрического резонатора имеет ярко выраженную немонотонную температурную зависимость. На рис. 2 наблюдаются несколько максимумов, соответствующих возбуждаемым колебательным модам в сегнетоэлектрическом резонаторе. С изменением температуры изменялись и резонансное магнитное поле, носившее скачкообразный характер, и добротность резонатора. Падение добротности соответствует нулевому значению в температурной зависимости увеличения соотношения сигнал/шум. Отметим, что при размещении образца ДФПГ вне сегнетоэлектрического резонатора

(но рядом с ним) увеличения чувствительности не наблюдалось.

## **2. Влияние сегнетоэлектрического резонатора на спиновое эхо**

Измерения проводились на импульсном радиоспектрометре (измененный спектрометр фирмы Вариан) с твердотельным предусилителем (100 mW) и усилителем (1 kW) микроволновой мощности трехсантиметрового (*X band*) диапазоне длин волн. Использовался резонатор типа петля-зазор. В этот резонатор при температуре 50 K помещался сегнетоэлектрический резонатор в виде трехгранной призмы, собранной из трех пластин, каждая размером  $0.5 \times 1.8 \times 4.0$  mm, из КТаO<sub>3</sub>. В зазор помещался образец — уголь. Чтобы избежать насыщения при нахождении образца в сегнетоэлектрическом резонаторе, с помощью аттенюатора было введено дополнительное поглощение мощности СВЧ 31 dB вместо обычно применяемого поглощения в 14 dB. Это соответствует ослаблению падающей на резонатор мощности в 50 раз. Последнее видно из следующего рассмотрения:

$$z = 10 \lg(P_0/P_n). \quad (1)$$

Здесь  $z$  — показания аттенюатора,  $P_0$  — мощность при  $z = 0$ ,  $P_n$  — мощность при введении аттенюатора. Для случаев измерений с сегнетоэлектрическим резонатором

$$z_{31} = 10 \lg(P_0/P_{\text{KT}_{301}}) \quad \text{и} \quad 10^{3.1} = P_0/P_{\text{KT}_{301}} \quad (2), (2a)$$

и без него имеем

$$z_{14} = 10 \lg(P_0/P), \quad 10^{1.4} = P_0/P. \quad (3), (3a)$$

Разделив (2а) на (3а), получаем уменьшение мощности, необходимой для регистрации сигнала, в 50 раз.

### 3. Интерпретация полученных результатов

Ниже предлагается метод использования расчетов диэлектрического резонатора правильной формы для выбора формы сегнетоэлектрического резонатора и оценки его размеров с целью его использования в ЭПР. Суть метода состоит в нахождении размеров сплошного сегнетоэлектрического резонатора (из того же материала), эквивалентного (в смысле резонансной частоты) сегнетоэлектрическому резонатору с отверстием для образца.

а) Расчет размеров прямоугольного сегнетоэлектрического резонатора для увеличения соотношения сигнал/шум. Рассчитаем резонансную частоту описанных выше сегнетоэлектрических резонаторов I и II, вырезанных из монокристаллического танталата калия. Заменим мысленно объем высверленной цилиндрической части  $V_c = \pi R^2 h$  сегнетоэлектрического резонатора объемом такой же величины, но формы прямоугольного параллелепипеда  $V_p = d^2 h$  и уменьшим длину и ширину резонатора на величину, равную  $d = \sqrt{\pi r^2}$ , где  $r^2 = R^2 h / L$  ( $L$  — длина резонатора). Тогда вместо  $2.85 \times 2.6 \times 3.4$  mm размер сегнетоэлектрического резонатора I составит  $1.63 \times 1.38 \times 3.4$  mm, а размер резонатора II вместо  $2.75 \times 3.5 \times 4.6$  mm будет составлять  $1.26 \times 2.01 \times 4.6$  mm.

При наличии в объемном резонаторе диэлектрического резонатора формы прямоугольного параллелепипеда резонансная частота последнего вычисляется из следующей системы уравнений [7]:

$$f = (\beta_x^2 + \beta_y^2 + \beta_z^2)^{1/2} c / (2\pi\epsilon^{1/2}),$$

$$\beta_z \operatorname{tg}(L\beta_z/2) = (\beta_x^2 + \beta_y^2 - \beta_0^2)^{1/2}, \quad (4)$$

где  $\beta_x = m\pi/A$ ,  $\beta_y = n\pi/B$ ,  $\beta_z = \pi\delta/L$ ,  $\beta_0 = 2\pi f/c$ ;  $A, B, L$  — длина, ширина и высота резонатора;  $m = n = 1$  — целые числа, соответствующие колебанию  $H_{111}$ ;  $\delta$  — часть полуволны внутри резонатора вдоль его высоты;  $c$  — скорость света;  $\epsilon$  — диэлектрическая проницаемость резонатора.

Расчет показал, что точное совпадение частоты получается при размере  $1.69 \times 1.439 \times 3.4$  mm и  $\delta = 0.833$  для резонатора I ( $\nu = 9150$  MHz) и при размере  $1.2 \times 1.958 \times 4.6$  mm и  $\delta = 0.877$  для резонатора II ( $\nu = 9124$  MHz). Именно при этих размерах усиление сигнала ЭПР оказывается наибольшим.

Результаты расчета указывают на возможность предлагаемым способом оценивать размеры сегнетоэлектрического резонатора для использования в измерениях ЭПР.

б) Влияние сегнетоэлектрического резонатора сферической формы на интенсивность сигнала ЭПР. Увеличение интенсивности сигнала ЭПР может быть описано выражением [A4] из [5], показывающим изменение напряженности магнитного поля на образце при размещении его внутри

сегнетоэлектрического резонатора сферической формы,

$$B_{ir}/B = C j_1(kr) \cos \theta/r. \quad (5)$$

Здесь  $B_{ir}$  — напряженность магнитного поля при наличии сегнетоэлектрического резонатора внутри объемного резонатора,  $B$  — напряженность магнитного поля в отсутствие сегнетоэлектрического резонатора,  $r$  — расстояние от центра сегнетоэлектрического резонатора до образца,  $j_1(x)$  — сферическая функция Бесселя первого порядка,  $C$  определяется по формуле

$$C = (a + D/a^2)/j_1(ka), \quad (6)$$

где  $D = a^3[((2\mu + 1)j_1(ka) - ka j_0(ka))/((\mu - 1)j_1(ka) + ka j_0(ka))]$ ;  $a$  — радиус сегнетоэлектрического резонатора;  $j_0(x)$  — сферическая функция Бесселя нулевого порядка;  $\mu$  — магнитная восприимчивость образца (мы принимаем, как в случае немагнитного объекта,  $\mu = 1$ ), волновое число  $k = (\mu\mu_0\epsilon_0\omega^2 - i\sigma\mu_0\omega)^{1/2}$ , где  $\epsilon$  — диэлектрическая проницаемость сегнетоэлектрического резонатора,  $\mu_0$  и  $\epsilon_0$  — магнитная и диэлектрическая проницаемость вакуума,  $\sigma$  — электрическая проводимость сегнетоэлектрического резонатора,  $\omega$  — угловая частота падающей СВЧ мощности.

Учитывая, что наш сегнетоэлектрический резонатор имеет очень низкую проводимость, мы полагаем  $\sigma = 0$ . Подставляя в выражение для  $k$  известные значения  $\mu_0$ ,  $\epsilon_0$  и  $\omega = 2\pi\nu$  ( $\nu = 9124$  MHz для сегнетоэлектрического резонатора II), получаем  $k = 192\sqrt{\epsilon}$  m<sup>-1</sup>.

Сферические функции Бесселя ( $n$ -го порядка) мы рассчитывали через разложение в ряд

$$j_n(ka) = \sum_{i=0}^{\infty} \frac{(-1)^i (ka/2)^{n+2i}}{i! \Gamma(n+i+1)}, \quad (7)$$

$\Gamma(n+i+1)$  — гамма-функция;  $\Gamma(n+i+1) = (n+i)!$

Учитывая слагаемые до 12-го порядка, мы получали хорошее согласие рассчитанных значений функции Бесселя со стандартными табличными значениями. Так, для  $j_1(kr)$  имеем

$$j_1(kr) = \frac{kr}{2 \cdot 1} \left( 1 - \frac{k^2 r^2}{2 \cdot 4} + \dots \right). \quad (8)$$

Видно, что при подстановке (8) в (5)  $r$  сокращается.

Для сегнетоэлектрического резонатора из КТаO<sub>3</sub> диэлектрическая проницаемость является комплексной величиной  $\epsilon = \epsilon' - i\epsilon''$ . Действительная часть  $\epsilon'$  зависит от температуры следующим образом:  $\epsilon' = 45 + 64000/(T - T_c)$ ,  $T_c = 4$  K [6]. Минимальная часть  $\epsilon'' = \epsilon' \operatorname{tg} \delta$ , где  $\operatorname{tg} \delta = 0.032$ .

Расчет  $B_{ir}/B$  при  $a = 0.77 \cdot 10^{-3}$  m дает максимум  $B_{ir}/B$  при  $T = 288$  K. Высота максимума составляет  $B_{ir}/B = 70$ . Этот расчет дает основание для дальнейшего увеличения интенсивности сигнала ЭПР за счет изменения формы сегнетоэлектрического резонатора.

#### 4. Заключение

Таким образом, использование сегнетоэлектрического резонатора в импульсном ЭПР позволяет уменьшить величину СВЧ мощности, необходимой для насыщения, и существенно повысить соотношение сигнал/шум в CW ЭПР. Отметим, что такое же повышение соотношения сигнал/шум достигнуто с помощью диэлектрического резонатора из сипфира [8] за счет оптимизации фактора заполнения резонатора. В нашем случае еще достаточно велик запас в дальнейшем повышении соотношения сигнал/шум за счет увеличения фактора заполнения резонатора.

Данная работа выполнена при частичной финансовой поддержке Фонда фундаментальных исследований Министерства науки и технологий Украины (проект № 2.4/516).

#### Список литературы

- [1] Hedvig P. Acta Physica Hungaricae. 1959. Vol. 10. N 1. P. 115–116.
- [2]. Karter D.L., Okaya A. // Phys. Rev. 1960. Vol. 118. N 6. P. 1485–1490.
- [3] Okaya A., Barach L.F. // Proc. IRE. 1962. Vol. 50. P. 2081–2092.
- [4] Yee H.Y. // IEEE Trans. MTT. 1965. Vol. 13. P. 256.
- [5] Sucki M., Rinard G.A., Eaton Sandra S., Eaton Gareth R. // J. of Magnetic Resonance. Ser. A. 1996. Vol. 118. P. 173–188.
- [6] Бузин И.М., Иванов И.В., Мусеев Н.Н., Чупраков В.Ф. // ФТТ. 1980. Т. 22. Вып. 7. С. 2057–2062.
- [7] Диэлектрические резонаторы // Под ред. М.Е. Ильчинко. М.: Радио и связь, 1989. 328 с.
- [8] Biehl R. // Bruker Report. 1986. N 1. P. 45.

Journal of Magnetic Resonance 153, 7–14 (2001)  
doi:10.1006/jmre.2001.2415, available online at <http://www.idealibrary.com> on IDEAL®

## Enhanced EPR Sensitivity from a Ferroelectric Cavity Insert

Yuri E. Nesmelov, Jack T. Surek, and David D. Thomas<sup>1</sup>

*Department of Biochemistry, University of Minnesota Medical School, Minneapolis, Minnesota 55455*

E-mail: ddt@umn.edu

Received January 23, 2001; revised July 24, 2001; published online October 5, 2001

We report the development of a simple ferroelectric cavity insert that increases the electron paramagnetic resonance (EPR) sensitivity by an order of magnitude when a sample is placed within it. The insert is a hollow cylinder (length 4.8 mm, outside diameter 1.7 mm, inside diameter 0.6 mm) made from a single crystal of  $\text{KTaO}_3$ , which has a dielectric constant of 230 at X-band (9.5 GHz). Its outside dimensions were chosen to produce a resonant frequency in the X-band range, based on electromagnetic field modeling calculations. The insert increases the microwave magnetic field ( $H_1$ ) at the center of the insert by a factor of 7.4 when placed in an X-band  $\text{TM}_{110}$  cavity. This increases the EPR signal for a small (volume 0.13  $\mu\text{L}$ ) unsaturated nitroxide spin label sample by a factor of 64 at constant microwave power, and by a factor of 9.8 at constant  $H_1$ . The insert does not significantly affect the cavity quality factor  $Q$ , indicating that this device simply redistributes the microwave fields within the cavity, focusing  $H_1$  onto the sample inside the insert, thus increasing the filling factor. A similar signal enhancement is obtained in the  $\text{TM}_{110}$  and  $\text{TE}_{102}$  cavities, and when the insert is oriented either vertically (parallel to the microwave field) or horizontally (parallel to the DC magnetic field) in the  $\text{TM}_{110}$  cavity. This order-of-magnitude sensitivity enhancement allows EPR spectroscopy to be performed in conventional high- $Q$  cavities on small EPR samples previously only measurable in loop-gap or dielectric resonators. This is of particular importance for small samples of spin-labeled biomolecules. © 2001 Academic Press

**Key Words:** electron paramagnetic resonance; ferroelectric;  $\text{KTaO}_3$ ; cavity insert; muscle fiber.

### INTRODUCTION

Improving the sensitivity (signal-to-noise ratio for a given sample) in EPR is particularly important for studying biological samples, which are often available only in limited amounts, particularly in analysis of protein mutants or single cells. In current EPR spectrometers, noise is constant and limited by the detector over a wide range of incident microwave power. Therefore, the goal of sensitivity enhancement is reduced to the task of increasing the signal intensity  $S$  at a constant number of spins. For the common case of a detector with a linear response, the signal

intensity  $S$  is given by (1)

$$S \propto \eta Q P^{1/2}, \quad [1]$$

where  $\eta$  is the filling factor,  $Q$  is the unloaded quality factor of the cavity, and  $P$  is the incident microwave power. In most EPR experiments, the power is adjusted to maximize signal intensity in the absence of saturation. For each sample, this condition is achieved at a characteristic value of the microwave magnetic field amplitude  $H_1$  at the sample, which is proportional to the square root of the incident power making the practical definition of sensitivity (relative signal at the optimal  $H_1$  and constant number of spins)

$$S \propto \eta Q H_1. \quad [2]$$

For most spectrometers and samples, it is easy to obtain a value of  $P$  high enough to achieve the optimal  $H_1$  value. Therefore, optimizing sensitivity is usually a matter of increasing  $Q$  or  $\eta$ . Most modern EPR cavities have been designed for optimally high  $Q$ , so our goal is to start with a commercial high- $Q$  cavity and to increase the filling factor  $\eta$ , which is given by (1)

$$\eta = (V_s \langle H_1^2 \rangle_s) / (V_c \langle H_1^2 \rangle_c), \quad [3]$$

where  $V_s$  and  $V_c$  are volumes of the sample and cavity, and  $\langle H_1^2 \rangle_s$  and  $\langle H_1^2 \rangle_c$  are the mean square microwave magnetic field values in the sample and cavity, respectively.

For the rectangular  $\text{TE}_{102}$  cavity ( $V_c \cong 10 \text{ cm}^3$ ), the filling factor is about  $2 V_s / V_c = 2 \times 10^{-4}$  for a 1- $\mu\text{L}$  “point” sample and  $V_s / V_c \cong 2 \times 10^{-3}$  for an optimal aqueous line sample (20  $\mu\text{L}$ ) (1). Noncavity resonators, such as loop-gap resonators (LGRs) or dielectric resonators (DRs), typically have filling factors 50–100 times greater than that of a  $\text{TE}_{102}$  cavity (3, 5), but a number of disadvantages limit the application of these devices. For example, a LGR has a low  $Q$  and can be difficult to tune. Its absorption spectrum is often distorted by a dispersion component, due to errors of phasing in the reference arm of the microwave bridge (6). Furthermore, most X-band EPR users already use cavities for biochemical measurements.

<sup>1</sup> To whom correspondence should be addressed.



Buying an LGR or DR can be as expensive as buying a new cavity because they can be difficult to manufacture (3, 4). Therefore, it is desirable to devise a means to increase the filling factor of a conventional resonant cavity.

It is possible to increase the filling factor by increasing the volume of the sample, but for aqueous samples this approach is severely limited by dissipative losses that can degrade  $Q$  and thus decrease  $S$  (Eq. [1]). Therefore, our goal is to redistribute  $H_1$  so that it is concentrated at the sample. There have been previous attempts to concentrate the  $H_1$  field at the sample by insertion of a resonant structure into a cavity, e.g., using a folded half-wave resonator (7) or a LGR (8). Even a quartz dewar (dielectric insert) increases  $H_1$  at the sample through such a perturbation. For a dielectric or ferroelectric insert,  $H_1$  at the sample increases in proportion to the square root of the dielectric constant ( $\epsilon$ ) of the insert material (1). This led to experimentation with low-loss microwave ceramics in resonators for EPR, with dielectric constants of about 30 (4) as well as low-loss ferroelectric materials that have constants of 100 to 300 (9, 10).

In the present study, we have investigated a crystalline ferroelectric,  $KTaO_3$ , for use as a hollow cylindrical insert in an X-band microwave cavity. Cylinder dimensions were calculated with mode matching (11-14) to produce an insert with an X-band resonant frequency. The microwave magnetic field  $H_1$  at the sample in the cavity with and without the insert was measured from the signals of EPR samples with known saturation properties, and the effect of the insert on EPR signal intensity was determined for samples of free spin-label solutions, spin-labeled lipids, and muscle fibers.

## METHODS

### Theoretical

Our goal was to fabricate an insert with a bore for the introduction of samples. We also wanted an insert with cylindrical symmetry, to ensure its excitability by the  $TE_{018}$  mode and to facilitate the calculation of microwave fields. Therefore, as a first approximation we designed the insert as a solid cylinder with an X-band resonant frequency. We used radial mode matching to compute the resonant frequency of the lowest order TE mode (11).

The computation starts with the well-known Helmholtz vector equation (12-14)

$$(1/r)d(r(d\Psi/dr))/dr - (m^2/r^2)\Psi + d^2\Psi/dz^2 + k_0^2\epsilon\Psi = 0, \quad [4]$$

where wavenumber  $k_0 = 2\pi/\lambda$  in air and  $k_0e^{1/2}$  in the cylinder insert. Here  $m = 0$  because of axial symmetry. Equation [4] is solved separately for regions I and II (Fig. 1) by separation of variables

$$\Psi = R(r)Z(z). \quad [5]$$

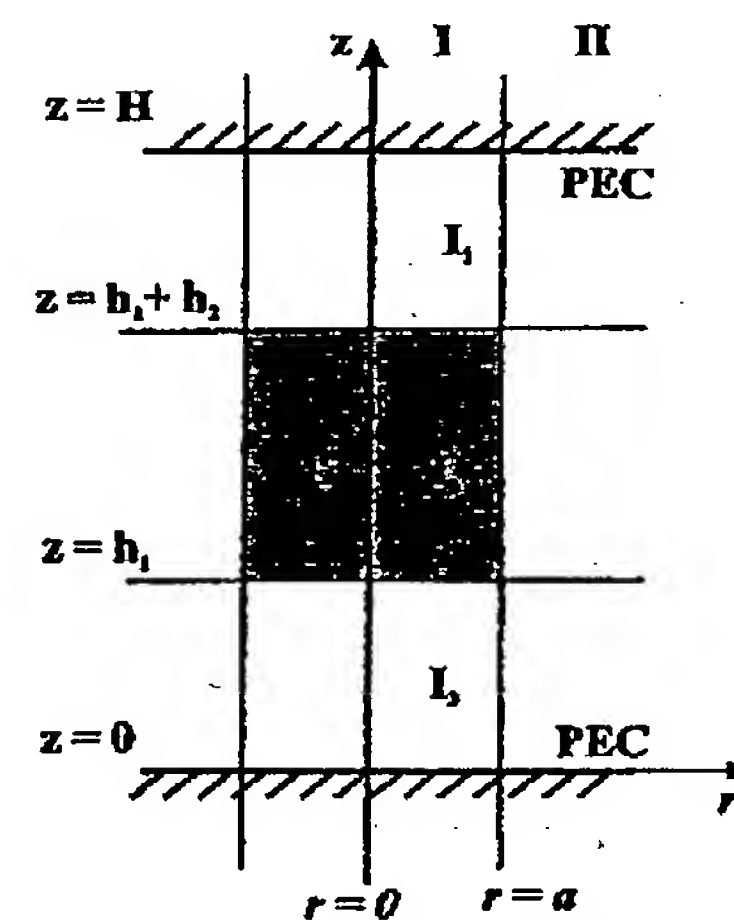


FIG. 1. Model of shielded solid cylindrical dielectric resonator. PEC is a perfect electric conductor.

We assume that most of the energy is stored in the insert and the microwave field decays exponentially in region II. Then, using Eq. [4] in region I,

$$(1/r)d(r(dR_1(r)/dr))/dr + p^2R_1(r) = 0 \quad [6]$$

$$d^2Z_1(z)/dz^2 + v^2Z_1(z) = 0, \quad [7]$$

and in region II,

$$(1/r)d(r(dR_2(r)/dr))/dr - q^2R_2(r) = 0 \quad [8]$$

$$d^2Z_2(z)/dz^2 + t^2Z_2(z) = 0, \quad [9]$$

where  $p^2$  and  $q^2$  are the eigenvalues and  $v^2 = k_0^2\epsilon - p^2$ ,  $t^2 = k_0^2 + q^2$ .

The solution of Eq. [6] is a Bessel function  $R_1(r) = J_0(pr)$  (we reject the solution  $R_1(r) = Y_0(pr)$  because it becomes infinite at  $r = 0$ ) as well as the solution of Eq. [8],  $R_2(r) = K_0(qr)$ .

The solution of Eq. [9] is  $Z_2(z) = \sin(tz)/t$  (we reject the solution  $Z_2(z) = \cos(tz)$  because  $\Psi = 0$  at  $z = 0$  and  $z = H$  due to boundary conditions). Then, because of boundary conditions  $\Psi = 0$  at  $z = 0$  and  $z = H$ ,  $tH = \pi n$  or  $t = \pi n/H$  and  $n = 1$  because we consider only the first low TE mode.

The solution of Eq. [7] for region I is more complicated because of layers with different dielectric constants of air and the insert and eigenfunction  $Z_1$  can be constructed as (12)

—in layer  $I_1$ ,

$$Z_{11}(z) = \sin(v_1 z)/v_1, \quad [10]$$

—in layer  $I_2$ ,

$$Z_{12}(z) = B \sin(v_2(z - h_1))/v_2 + C \cos(v_2(z - h_1)), \quad [11]$$

## FERROELECTRIC EPR CAVITY INSERT

9

—in layer  $J_3$ ,

$$Z_{13}(z) = D \sin(v_1(z - H))/v_1, \quad [12]$$

where  $B = \cos(v_1 h_1)$ ,  $C = (\sin(v_1 h_1)/v_1)$ , and  $D = \cos(v_2 h_2) - (v_2/v_1)(\sin(v_1 h_1)/\cos(v_1 h_1)) \sin(v_2 h_2)$ . The insert is in the center of a cavity, which means that  $h_1 = H - (h_1 + h_2)$ . The continuity of tangential fields of region I requires that  $Z_{11} = Z_{12}$  at  $z = h_1$ ,  $Z_{12} = Z_{13}$  at  $z = h_1 + h_2$ , and  $dZ_{11}/dz = dZ_{12}/dz$  at  $z = h_1$ ,  $dZ_{12}/dz = dZ_{13}/dz$  at  $z = h_1 + h_2$ . Then, from Eqs. [10]–[12],

$$2(v_2/v_1)\operatorname{tg}(v_1 h_1) + \operatorname{tg}(v_2 h_2)\{1 - (v_2/v_1)^2 \operatorname{tg}^2(v_1 h_1)\} = 0. \quad [13]$$

A fundamental property of these solutions is that the eigenvalues  $p^2$  are less than  $k_0^2 \epsilon$  (13, 14). We need to find only the first eigenvalue because we compute the resonant frequency for only the first low TE mode.

When eigenvalues  $p^2$  and  $q^2$  are found, the resonant frequency is found by matching the tangential microwave fields at the boundary between regions I and II. The fields  $H_\phi = E_z = E_r = 0$  (13) and tangential microwave fields can be expressed as

$$\begin{aligned} H_z &= -\{d^2\Psi/dz^2 + k_0^2 \epsilon \Psi\}, \\ E_\phi &= d\Psi/dr. \end{aligned} \quad [14]$$

Regions I and II is boundary conditions

$$\begin{aligned} H_z^I &= H_z^{II} \text{ at } r = a, \\ E_\phi^I &= E_\phi^{II} \text{ at } r = a \end{aligned}$$

give the equation

$$J_0(pa)/J_1(pa) = -(q/p) K_0(qa)/K_1(qa), \quad [15]$$

which must be solved to determine the frequency of resonance.

The resonance frequency of our cavity is  $\nu = 9.316$  GHz, and the dimensions of the insert calculated by this method were  $h_2 = 3.85$  mm and  $2a = 1.76$  mm at this frequency. The relative dielectric constant of the  $\text{KTaO}_3$  crystal was assumed to be  $\epsilon = 230$  at 10 GHz (15). A hole was drilled down the axis for sample loading, assuming that this does not affect the resonance frequency substantially. We guessed that this perturbation could be compensated with a slight increase in value of the insert height  $h_2$ . The final dimensions were 4.8 mm in height with 1.76 mm as outside diameter and 0.6 mm as inside diameter. The value  $2a = 1.76$  mm is an average value; the insert has a slightly conical shape, with a difference of 0.04 mm between the diameters of the ends. The axis of the insert was made parallel to the [100] axis of a  $\text{KTaO}_3$  crystal (although the dielectric constant is specified to be isotropic for this crystal). The insert was centered with its axis perpendicular to the external magnetic field in the

TE and TM cavities and parallel to the external magnetic field for the transverse orientation for the TM cavity.

### Experimental

EPR experiments were performed with a Bruker EleXsys E500 spectrometer (Bruker Instruments Inc., Billerica, MA), using either (1) a  $\text{TE}_{102}$  cavity (model 4102 ST; Bruker Instruments Inc.) with a quartz dewar, (2) a  $\text{TM}_{110}$  cavity (model 4103 TM; Bruker Instruments Inc.) with no dewar, or (3) a loop-gap resonator (Medical Advances, Milwaukee, WI) with an external dewar. In all cases the axis of the sample tube and the insert was placed vertically, perpendicular to the DC magnetic field  $H_0$  and parallel to the microwave magnetic field  $H_1$ , except in the case of the TM cavity, which was modified to place the axis either parallel or perpendicular to the DC magnetic field (16). The temperature was controlled at 23°C using a nitrogen gas-flow temperature controller, and monitored with a digital thermometer using a SensorTek (Clifton, NJ) IT-21 thermocouple microprobe inserted into the top of the sample capillary, such that it did not affect the EPR signal. The spectra were acquired using 100 kHz field modulation. Peak-to-peak modulation amplitude was 0.01 G for measurements of the distribution of signal intensity vs position along the cavity axis with a BDPA point sample, 0.5 G at measurement of saturation rollover curves, 2 G at measurement of lipid sample, and 3 G at muscle fiber sample measurements. All investigated samples were loaded into fused quartz round capillaries with 0.4 mm ID, 0.55 mm OD (Vitro Dynamics Inc., Rockaway, NJ). Crystals of  $\text{KTaO}_3$  were obtained as a gift from Dr. L. A. Boatner (Oak Ridge National Laboratory, TN). The quality factors  $Q$  of the unloaded cavity with and without the insert were measured with an HP 8510C Network Analyzer and found as the ratio of resonance frequency to dip linewidth, measured at –3 dB from the baseline.

The microwave magnetic field amplitude  $H_1$  at the sample was calibrated by measuring the half-saturation power  $P(1/2)$  of 0.9 mM deoxygenated peroxylamine disulfonate (PADS) in 10 mM  $\text{K}_2\text{CO}_3$  aqueous solution (2). The relationship between  $H_1$  and incident power is given by the equation

$$H_1 = CP^{1/2}. \quad [16]$$

The constant  $C$  incorporates the effect of quality factor ( $Q$ ) and filling factor ( $\eta$ ).  $\text{TE}_{102}$  and  $\text{TM}_{110}$  cavities typically have  $C \approx 1 \text{ G/W}^{1/2}$ , while LGRs and DRs typically have  $C \approx 4–5 \text{ G/W}^{1/2}$ . To determine power at half-saturation, the dependence of signal intensity on the square root of incident power (saturation rollover curve) was obtained as shown in Fig. 2.  $H_1$  at half-saturation for PADS is 0.1067 G (2); the ratio of this  $H_1$  to the square root of the corresponding incident power gives  $C$ . Knowing  $C$  allows the field  $H_1$  at the sample to be related to the incident power. The constants  $C$  for  $\text{TE}_{102}$  with dewar and for  $\text{TM}_{110}$  are shown in Table 1 in the column marked as  $C_0$ .

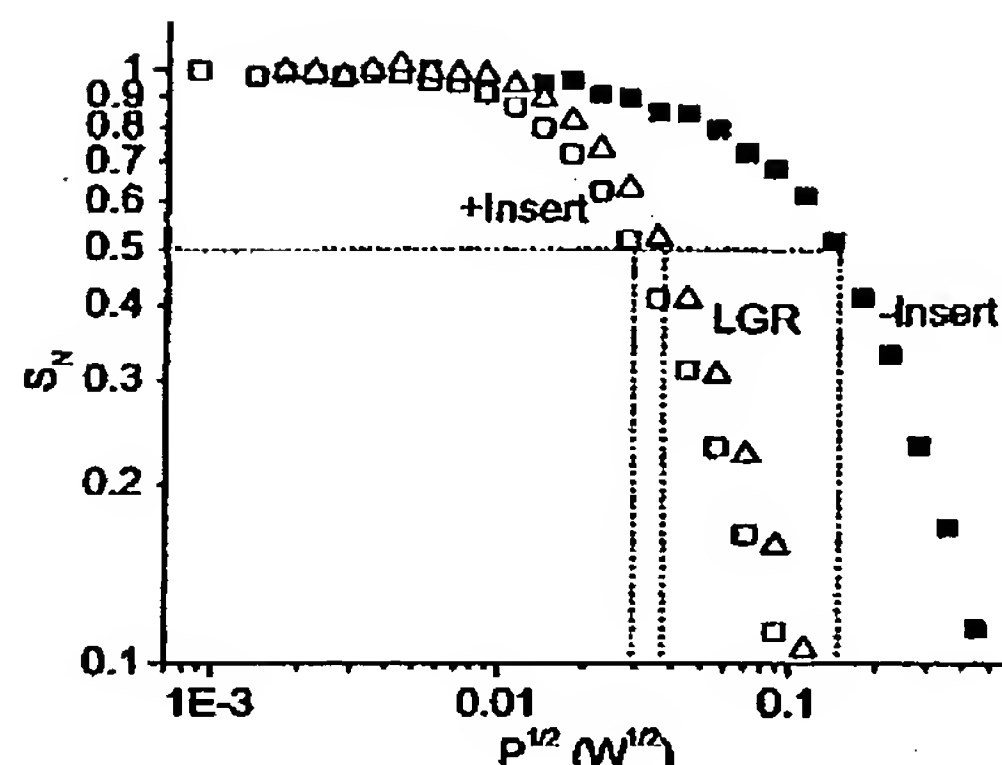


**FIG. 2.** Saturation rollover curves for 100  $\mu\text{M}$  IASL aqueous solution for the  $\text{TE}_{102}$  cavity without (filled squares) and with the insert (open squares) and the LGR (open triangles).  $P$  is the incident microwave power.  $S_N$  is the signal intensity normalized so that a value of 1 indicates no saturation (signal proportional to  $P^{1/2}$ ); i.e.,  $S_N = (S(P)/P^{1/2})/(S(P_0)/P_0^{1/2})$ , where  $P_0$  is a nonsaturating power.

For simplicity,  $H_1$  calibrations at the sample for cavities with and without the insert and for the LGR were made with a 100  $\mu\text{M}$  IASL aqueous solution. The saturation behavior of a sample that has IASL free in solution is determined solely by the relaxation properties of IASL and should be the same in different resonators, with and without the insert. Saturation rollover curves for the  $\text{TM}_{110}$  cavity with and without the insert in perpendicular and parallel orientations and for the  $\text{TE}_{102}$  cavity with and without the insert in perpendicular orientation were obtained. Constants  $C$  for the different cases were then determined and are shown in the Table 1. Figure 2 shows examples of saturation rollover curves of 0.2  $\mu\text{L}$  of 100  $\mu\text{M}$  IASL aqueous solution in the  $\text{TE}_{102}$  cavity with and without the insert and in the LGR.

The following reagents and solutions were used in this study: peroxylamine disulfonate (PADS), free radical BDPA complex with benzene ( $\alpha, \gamma$ -bisdisiphenylene- $\beta$ -phenylallyl), 4-(2-iodoacetamido)-2,2,6,6-tetramethyl-1-piperidinyloxy (IASL), TEMPO, and 4',4-dimethyloxazolidine-5-oxyl derivative of stearic acid (5-SASL) (all Aldrich Chemicals Co., Milwaukee, WI), and diolcoylphosphatidylcholine (DOPC) lipids (Avanti Polar Lipids, Alabaster, AL).

**Lipid sample preparation.** DOPC and 5-SASL (100/1) were mixed in chloroform, and the solvent was removed under a stream of nitrogen gas that left the lipid sample deposited as a thin layer at the bottom of a glass test tube. Chloroform traces were removed under vacuum. The dried lipid sample was then rehydrated with MOPS buffer (pH 7.0), pipetted into a capillary flame-sealed on one end, and then concentrated by centrifuging at 100,000 rpm for 30 min. After removing the excess liquid, the sample length was 1.7 mm; the quantity of 5-SASL in the sample was 0.4 nmoles.

**Muscle sample preparation.** Psoas muscle from New Zealand white rabbits was dissected, glycerinated, and spin-

labeled specifically at Cys 707 (SH1) with IASL in rigor buffer (130 mM potassium propionate, 20 mM MOPS, 1 mM EDTA, 2 mM MgCl<sub>2</sub>, 1 mM NaN<sub>3</sub>) as described elsewhere (17). After labeling, the fiber bundles were washed in a mixture of 50% glycerol and 50% rigor buffer. A muscle fiber bundle with diameter 0.15 mm and length 4 mm was placed in a capillary and held isometrically by suture tied to the bundle ends. The capillary was filled with a mixture of 50% glycerol and 50% rigor buffer and sealed with Critoseal at both ends.

## RESULTS

Introducing the insert into the cavity increased the EPR signal substantially, without increasing the noise. For example, the signal intensity from an unsaturated point sample of BDPA, placed in the center of a TE cavity, was increased by a factor of 45 (Fig. 3). This factor was even greater for a TM cavity: 80 if the insert was perpendicular to the DC field (Fig. 4) and 67 if the

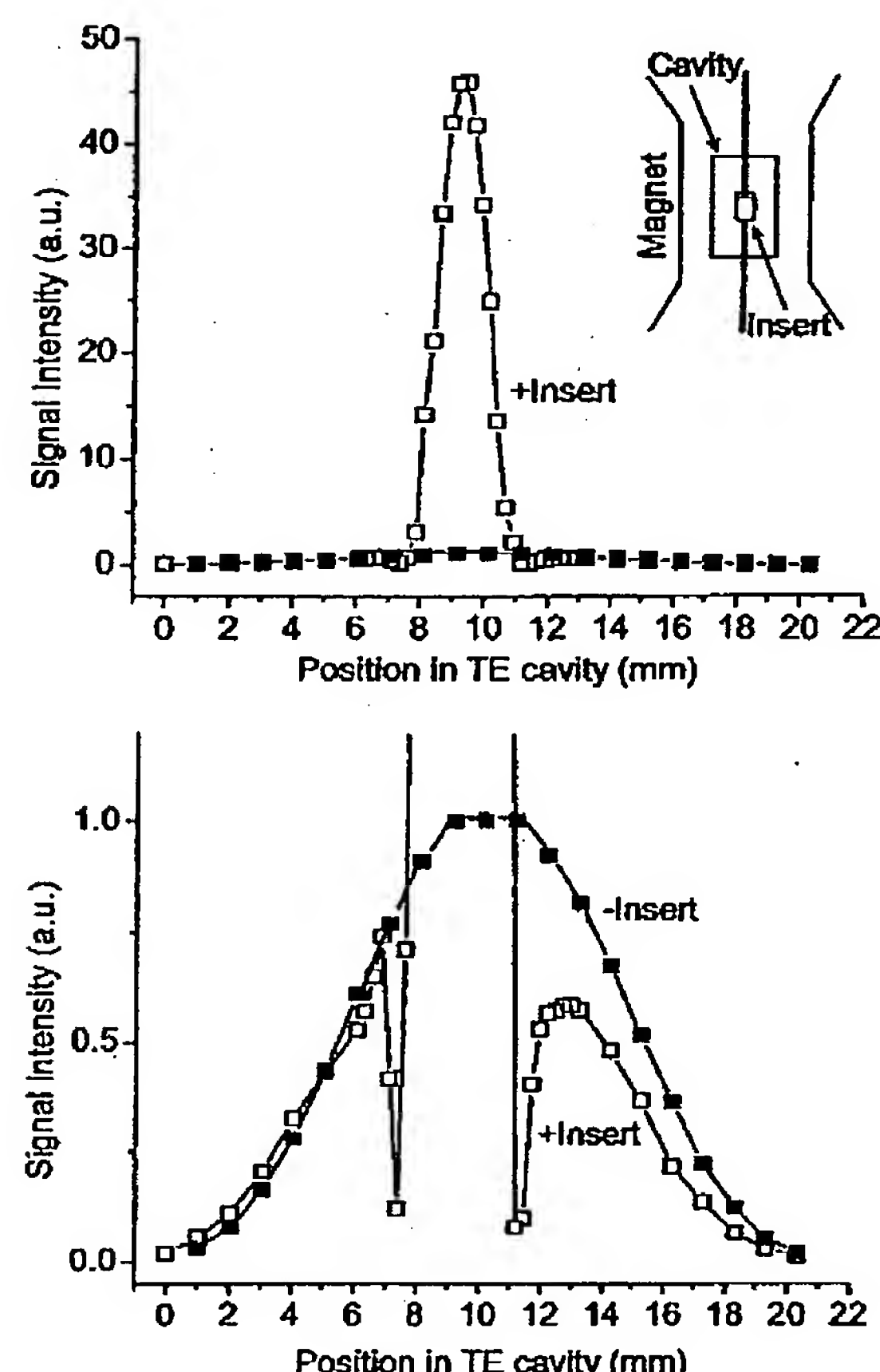


**FIG. 3.** Distribution of signal intensity of a point BDPA sample along the vertical axis (perpendicular to the DC magnetic field) of the  $\text{TE}_{102}$  cavity without (-Insert) and with the insert (+Insert).

## FERROELECTRIC EPR CAVITY INSERT

11

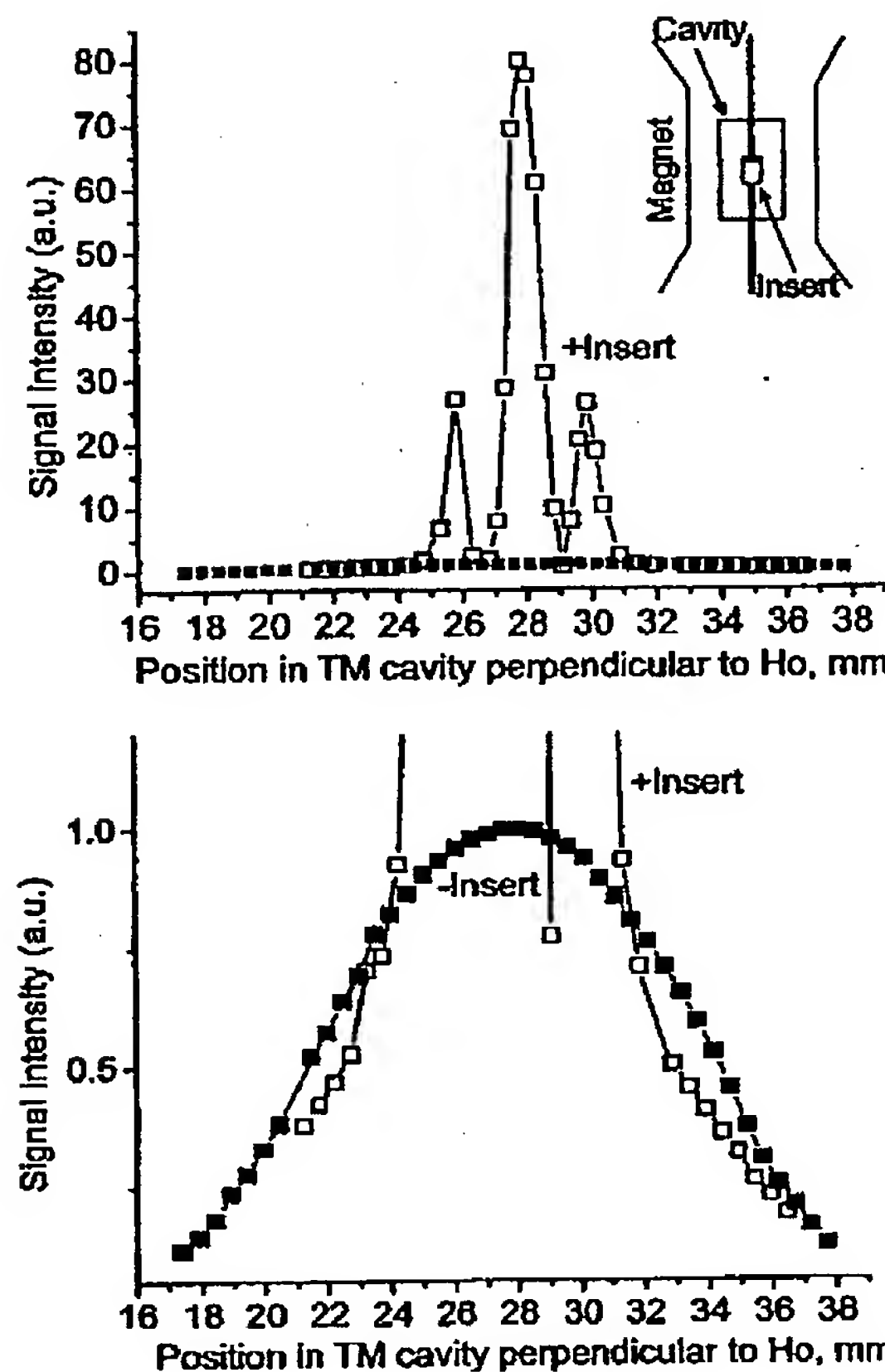


FIG. 4. Distribution of signal intensity of a point BDPA sample along the vertical axis (perpendicular to the DC magnetic field) of the  $\text{TM}_{110}$  cavity, without (filled squares) and with the insert (open squares).

insert was parallel to the DC field (Fig. 5). Figures 3, 4, and 5 show the dependence of signal intensity on the position of this point sample along the cavity axis, normalized to the signal at the center of the cavity in the absence of the insert. The asymmetry in Figs. 3, 4, and 5 is probably due to imprecise centering of the insert in the cavity or imperfection in its cylindrical shape (see Introduction).

Figure 6 shows the spectrum of  $0.6 \mu\text{L}$  of  $10 \mu\text{M}$  TEMPO spin label in a cavity with the insert (raw), a baseline (spectrum of cavity with the insert and with the same amount of distilled water replacing the TEMPO), and the spectrum resulting from subtraction of the baseline from the TEMPO spectrum. The baseline of the cavity with the insert shows a weak EPR line with  $g = 2.004$  and a peak-to-peak linewidth of 12 G. The EPR signal of the insert probably corresponds to trace  $\text{Fe}^{3+}$  ions (18, 19).

A comparison of the performance of the TE cavity with insert and the LGR for  $0.2 \mu\text{L}$  of  $10 \mu\text{M}$  aqueous TEMPO at the same incident power shows that the LGR produces a more intense signal; the ratio of signal intensities of the same sample in the LGR and in the TE cavity with the insert is 2.2.

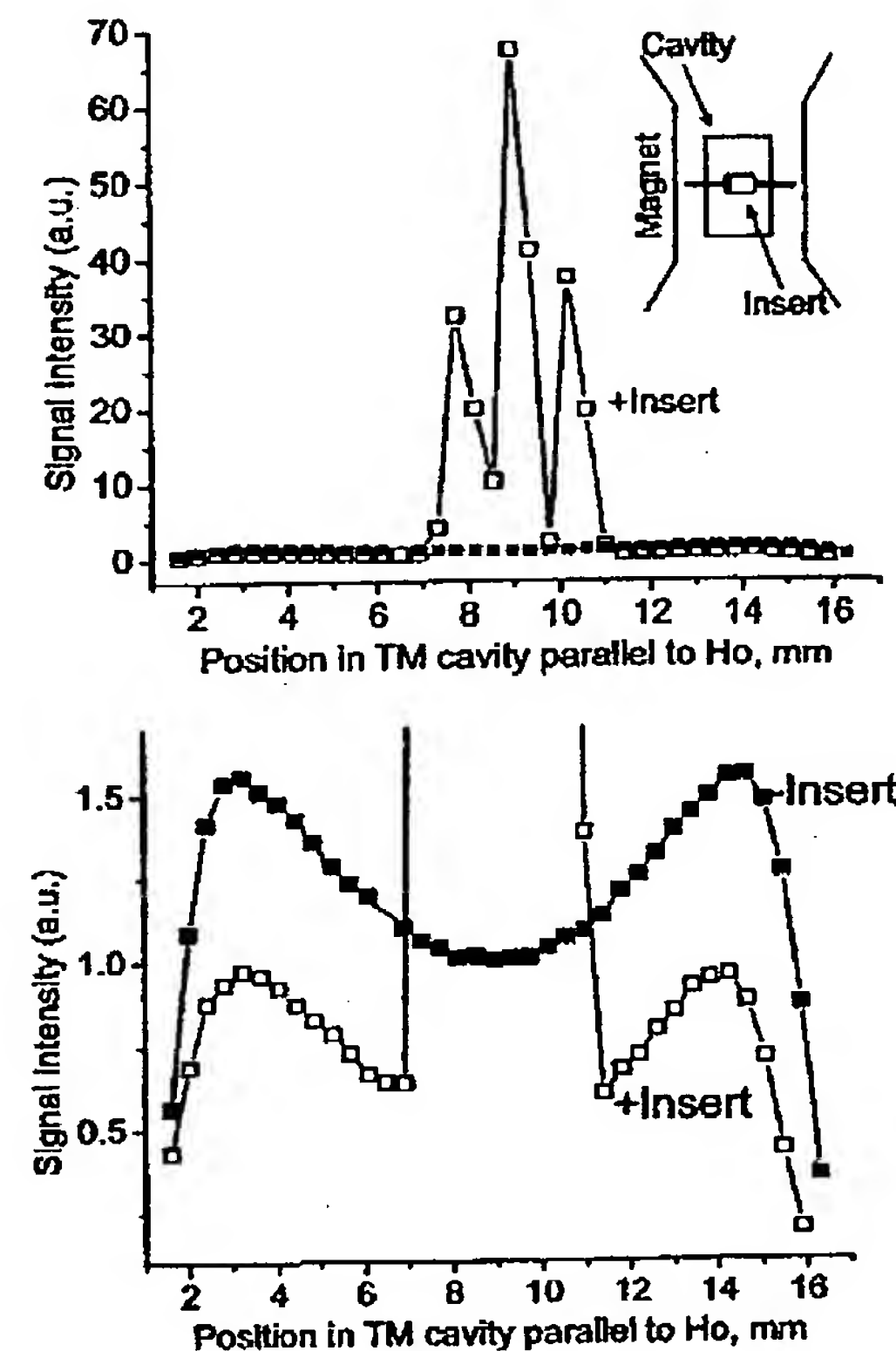


FIG. 5. Distribution of signal intensity of point BDPA sample along the horizontal axis (parallel to DC magnetic field) of the  $\text{TM}_{110}$  cavity, without (filled squares) and with the insert (open squares).

We found a shift in the frequency of resonance when the insert is placed in the cavity. For the TE cavity, the resonance frequency changed from 9.316 to 9.361 GHz, for the TM cavity from 9.801 to 9.809 and 9.804 GHz in the perpendicular and parallel insert orientations, respectively.

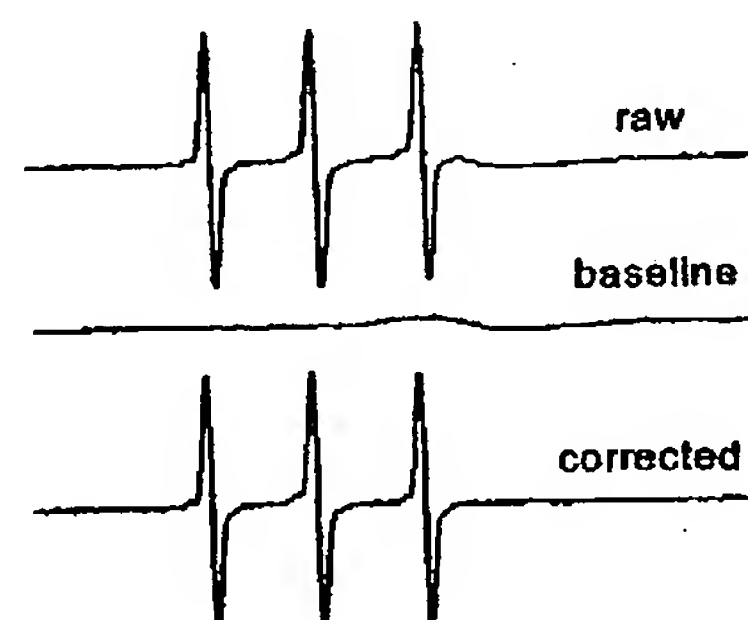


FIG. 6. EPR spectra for baseline subtraction acquired for  $0.6 \mu\text{L}$  of  $10 \mu\text{M}$  TEMPO aqueous solution. Experimental conditions: gain 80 dB (2e5),  $P = 0.63$  mW, time constant 41 ms, sweep 120 G/42 s, 25 scans acquired for each trace.

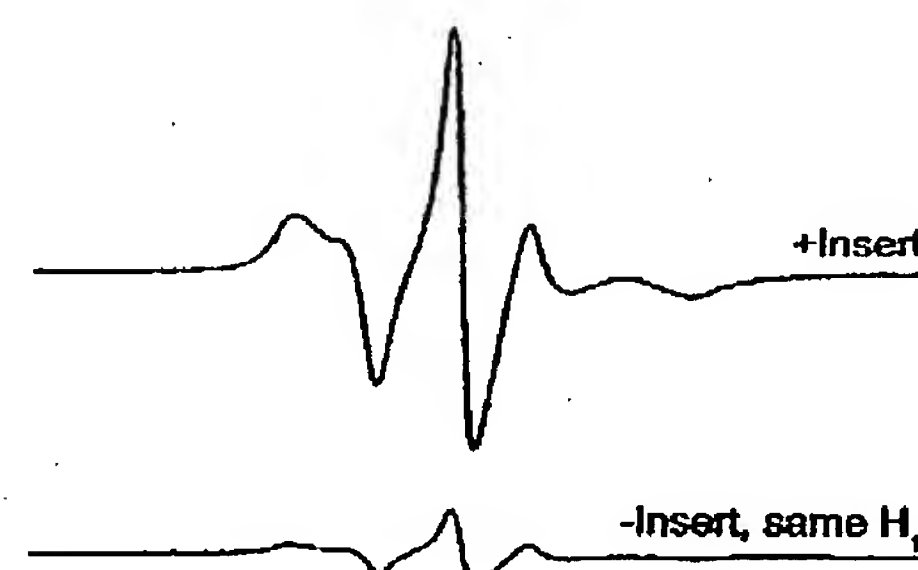


FIG. 7. EPR spectra acquired for a lipid sample: fatty acid spin label 5-SASL in DOPC lipids. The quantity of 5-SASL in the sample is approx. 0.4 nmoles. In the TE cavity with the insert,  $P = 0.63$  mW,  $H_1 = 123$  mG (top). In the TE cavity without the insert,  $P = 15.94$  mW,  $H_1 = 121$  mG (bottom). Sample length, 2.2 mm; volume, 0.3  $\mu$ L. Experimental conditions: gain 80 dB (2e5), time constant 41 ms, sweep 110 G/42 s, 30 scans acquired for each trace.

We observed dramatic amplifications of EPR spectra without significant distortion when the ferroelectric insert bore was loaded with lossy aqueous samples in all orientations. This is strong evidence that the microwave magnetic and electric fields remain spatially well separated between the insert bore and sidewall, respectively. We also found no shift in resonance frequency between an empty bore and one with a lossy sample loaded in all orientations. This means the power loss due to the interaction of the microwave electric field with the aqueous (muscle fiber) sample is small.

Enhancement of EPR signals of biological samples by the insert, at constant  $H_1$ , is shown in Figs. 7, 8, and 9. Figure 7 shows the EPR spectra of 5-SASL in DOPC lipid bilayers in the TE cavity. Figures 8 and 9 show the EPR spectra of a muscle fiber bundle perpendicular and parallel to the external magnetic field mounted in the TM cavity. The enhancement for fatty acid spin label in lipid bilayers in the TE cavity is 6.4 (Fig. 7). The enhancement for a spin-labeled muscle fiber handle in the TM cavity is 4.7 when the insert and fiber are placed perpendicular

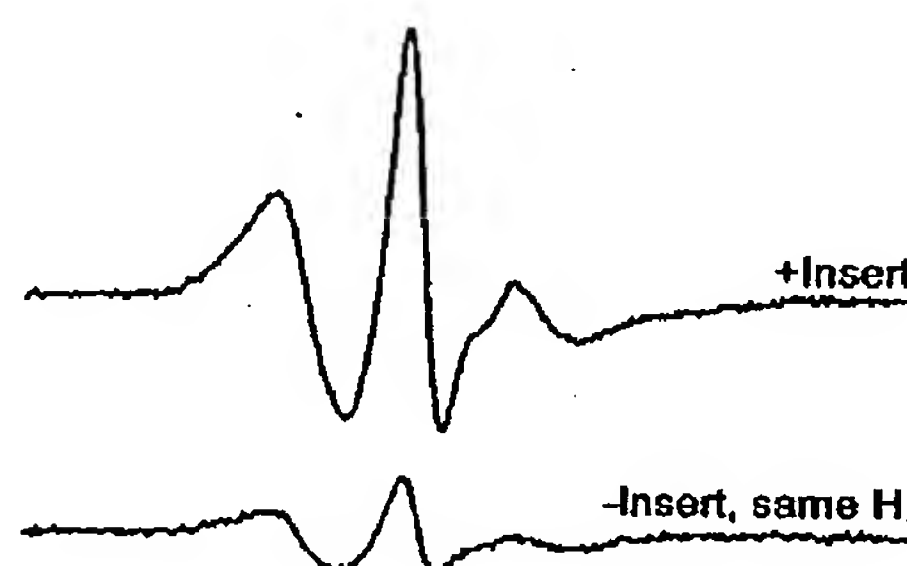


FIG. 8. EPR spectra recorded for a muscle fiber bundle in perpendicular orientation spin labeled at Cys707 of myosin head (SH1) by IASL. In the TM cavity with the insert,  $P = 0.63$  mW,  $H_1 = 138$  mG, baseline subtracted (top). In the TM cavity without the insert,  $P = 31.81$  mW,  $H_1 = 139$  mG (bottom). Experimental conditions: gain 80 dB (2e5), time constant 41 ms, sweep 120 G/42 s, 20 scans acquired for each trace.

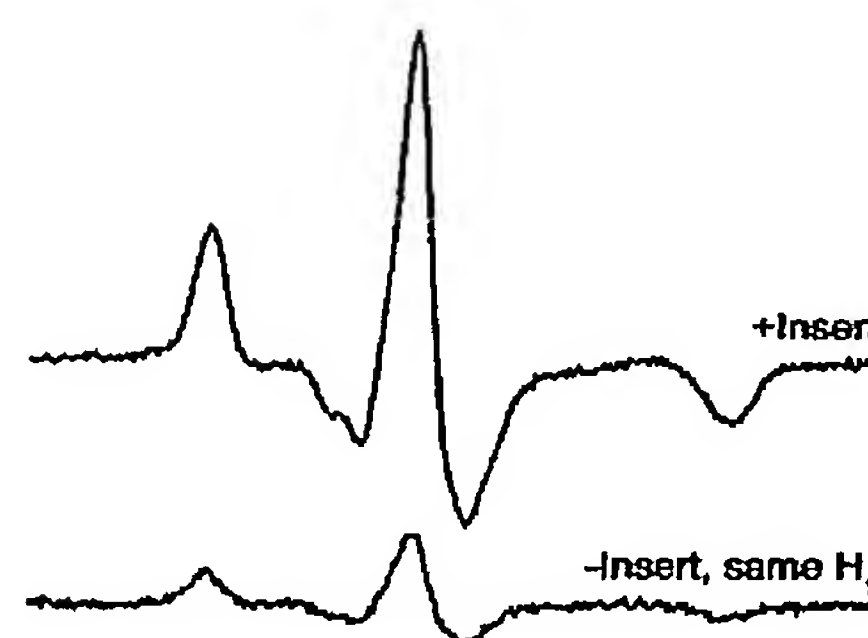


FIG. 9. EPR spectra recorded for a muscle fiber bundle in parallel orientation spin labeled at Cys707 of myosin head (SH1) by IASL. In the TM cavity with the insert,  $P = 0.63$  mW,  $H_1 = 146$  mG, baseline subtracted (top). In the TM cavity without the insert,  $P = 31.81$  mW,  $H_1 = 139$  mG (bottom). Experimental conditions: gain 80 dB (2e5), time constant 41 ms, sweep 120 G/42 s, 20 scans acquired for each trace.

to DC field and 4.5 when the orientation of the insert and fiber are parallel to the DC field.

Table 1 illustrates the effect of the insert on  $H_1$  and signal intensity for various samples and cavities. The first and second columns give values of conversion factor  $C_0$  for the cavity without the insert and  $C$  for the cavity with the insert, where  $C$  is the ratio of  $H_1$  and  $P^{1/2}$  (Eq. [16]). The third column presents the ratio of conversion factors  $C/C_0$ , which is the ratio of  $H_1$  at the sample in the cavity with and without the insert at the same incident power. The last four columns show ratios of signal intensities of different samples in cavities with and without the insert at the same  $H_1$  or at the same incident power, under unsaturated conditions. Samples were centered simultaneously in the cavity and the insert. The point sample was a tiny piece of BDPA. The aqueous samples were 1 mM TEMPO, 0.2  $\mu$ L ( $l = 1.7$  mm) for the TE cavity and 0.13  $\mu$ L ( $l = 1$  mm) for the TM cavity. The different volumes were chosen to completely fill only the central part of the microwave magnetic field distribution found throughout the insert (see Figs. 3–5). Column eight shows ratios of integral intensity of signals of the muscle fiber bundle sample in the cavity with and without the insert at the same  $H_1$  at the sample.

## DISCUSSION

### *Enhancement of Signal Intensity and Filling Factor of a Cavity with the Insert*

As indicated in the discussion of Eq. [1] in the Introduction, EPR sensitivity for a given sample is proportional to the quality factor  $Q$  and the filling factor  $\eta$ . We found that the ferroelectric insert had no significant effect on  $Q$ , so the improvement in signal intensity with the insert is found to be directly proportional to the increased filling factor

$$(S/S_0)_P \propto (\eta/\eta_0), \quad [17]$$

## FERROELECTRIC EPR CAVITY INSERT

13

TABLE 1

Cavity/insert orientation	$C_0^a$ (G/ $\sqrt{W}$ )	$C^b$ (G/ $\sqrt{W}$ )	$C/C_0^c$	Signal intensity ratio <sup>d</sup>			Muscle fiber <sup>e</sup> , same $H_1$ (S/S <sub>0</sub> ) <sub>H<sub>1</sub></sub>
				Point sample <sup>f</sup> , same power (S/S <sub>0</sub> ) <sub>P</sub>	Aqueous sample <sup>f</sup> Same power (S/S <sub>0</sub> ) <sub>P</sub>	Same $H_1$ (S/S <sub>0</sub> ) <sub>H<sub>1</sub></sub>	
TE	0.96	4.7	4.9	45	34 <sup>h</sup>	7 <sup>h</sup>	
TM/perpendicular	0.78	5.8	7.4	80	64 <sup>i</sup>	9.8 <sup>i</sup>	4.7
TM/parallel	0.78	5.5	7	67	56 <sup>i</sup>	8.5 <sup>i</sup>	4.5

<sup>a</sup> Cavity conversion factor ( $C = H_1/P^{1/2}$ ) without insert.<sup>b</sup>  $C$  with insert.<sup>c</sup> Increase of  $H_1$  at the sample in cavity with the insert.<sup>d</sup> Ratio of signal intensities of sample in cavity with and without insert.<sup>e</sup> BDPA.<sup>f</sup> 1 mM TEMPO aqueous solution.<sup>g</sup> Four millimeter muscle fiber bundle labeled by IASL at Cys707 of SH1.<sup>h</sup>  $V = 0.2 \mu\text{L}$ ,  $l = 1.7 \text{ mm}$ .<sup>i</sup>  $V = 0.13 \mu\text{L}$ ,  $l = 1 \text{ mm}$ .

where 0 indicates the absence of the insert. Both signals  $S$  and  $S_0$  are measured under unsaturated conditions. For fixed volumes of sample and cavity, and considering Eq. [3], we conclude that the improvement of signal intensity reflects the redistribution of the microwave field  $H_1$  in the cavity by the insert, such that more of the available magnetic field  $H_1$  is focused on the sample.

The difference in the signal intensities for a point sample and for an aqueous sample in Table 1 can be explained by the variation in microwave magnetic field strength along the axis of the linear sample covered by the insert compared with a constant and maximal field  $H_1$  for the point sample in the center of the insert (Figs. 3–5). Thus the peak field  $H_1$  detected with a point sample in the center of the insert is larger than the average field  $H_1$  throughout the insert for a 1.7-mm (TE) and 1-mm (TM) long line sample. Also, a 4-mm muscle fiber sample shows an even lower signal intensity ratio, as it extends a significant length from the center of the insert, where  $H_1$  has a maximum value.

According to Eq. [17], the signal intensity ratio is proportional to the ratio of filling factors for the cavity with and without the insert. Then, from Eq. [16],

$$(S/S_0)_{H_1} \propto (\eta/\eta_0)(C_0/C) = (S/S_0)_P(C_0/C), \quad [18]$$

where  $(S/S_0)_{H_1}$  is the signal intensity ratio at the same  $H_1$ , and  $(S/S_0)_P$  is the signal intensity ratio at the same incident power. This equation can be tested precisely for the aqueous sample, since it is for this sample that the effective  $H_1$  value is accurately calibrated. The data in Table 1 are in excellent agreement with Eq. [18] for the TE cavity (calculated  $(S/S_0)_{H_1}$  is  $34 \cdot (4.9)^{-1} = 6.9$ , observed is 7.0), agreement is also good for TM/perpendicular (calculated  $(S/S_0)_{H_1}$  is  $64 \cdot (7.4)^{-1} = 8.7$ , observed is 9.8), and for the TM/parallel (calculated  $(S/S_0)_{H_1}$  is  $56 \cdot (7)^{-1} = 8.0$ , observed is 8.5). The small deviations are probably due to the 1-dB precision of the power setting, which

limits the ability to achieve precisely the same  $H_1$  for different  $C$  values, to nonuniform  $H_1$  over the finite length of the sample, and/or to imprecise positioning of the sample in the center of the cavity.

The observed dramatic improvement of  $H_1$  and signal intensity at the sample shows that there is a strong distributed coupling (8) between the insert and the cavity. In the frequency range from 9.1 to 9.9 GHz, only one resonance is observed, confirming the strong coupling of the insert to the cavity.

In the presence of the insert, there are two sharp minima of signal intensity in Figs. 3–5. For the TE cavity, the distance between these minima is 3.9 mm, which is in good agreement with the length of the resonator, as calculated from the solid cylindrical resonator model (3.85 mm). In a cylindrical insert the microwave magnetic field measured along the axis should have a maximum value in the center and minimum values at the ends, reflecting the boundary conditions. Thus the minima of signal intensity can be explained as nodes of a standing wave formed in the insert. This agreement between the model of a solid cylindrical resonator of  $\text{KTaO}_3$  and the real cylindrical insert, which has an axial hole, confirms that the hole does not change the resonance conditions of the insert in cavity very much.

#### Performance of a Cavity with the Insert vs a Loop-Gap Resonator

The strengths of a LGR are a much greater filling factor  $\eta$  and much higher  $C_0$  (i.e.,  $H_1/P^{1/2}$ ), compared with those of a cavity. The LGR increases  $H_1$  by a factor of 8.2 compared to a cavity for the same incident power (3). For a 1- $\mu\text{L}$  sample in a capillary with 0.6 mm ID, the filling factor  $\eta$  is about 0.29 in a LGR (20), compared with  $2 \times 10^{-4}$  in a  $\text{TE}_{102}$  cavity (1). This high value of the filling factor more than compensates for the low-quality factor  $Q$  of the LGR (600–800, compared with

**IN THE UNITED STATES PATENT AND TRADEMARK OFFICE**

APPLICANT(S): Geifman et al

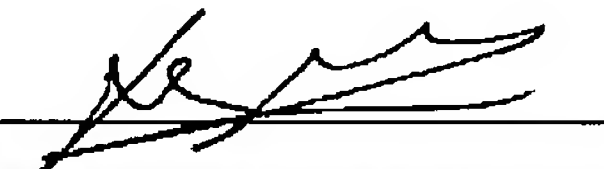
SERIAL NO.: 10/605,251

FILING DATE: September 18, 2003

TITLE: Ferroelectric Single Crystal Resonator And Methods For Preparation And Use Thereof

**CERTIFICATE OF TRANSMISSION/ MAILING UNDER 37 C.F.R. 1.8**

I hereby certify that this correspondence, and any document(s) referred to as enclosed herein, is/are being facsimile transmitted to the USPTO or deposited with the United States Postal Service as first class mail, postage prepaid, in an envelope addressed to the Commissioner for Patents, P.O. Box 1450, Alexandria, VA 22313-1450 on this 12 day of April 2004.

  
Leonid Khodor

Commissioner for Patents  
P.O. Box 1450,  
Alexandria, VA 22313-1450

Sir:

Submitted herewith is/are:

1. Transmittal Form;
2. Copy of IDS Citation "I.N. Geifman, I.S. Golovina, E.R.Zusmanov, V.I. Kofman "Увеличение чувствительности спектрометра электронного парамагнитного резонанса с помощью сегнетоэлектрического резонатора", Журнал технической физики, 2000, Том. 70, вып. 2" - 4 pages.
3. Copy of IDS Citation "Yuri E. Nesmelov, Jack T. Surek, and David D. Thomas "Enhanced EPR Sensitivity from a Ferroelectric Cavity Insert", Jurnal of Magnetic Resonance, 153,7-14 (2001)" -7pages.